Contrib Mineral Petrol (1992) 112:358–370

Contributions to Mineralogy and Petrology

Ultra-high temperatures from oxygen isotope thermometry of a coesite-sanidine grospydite

Z.D. Sharp [1], E.J. Essene [1, 2], and J.R. Smyth [3]

[1] Institut de Minéralogie et de Pétrographie, Université de Lausanne, BFSH-2, CH-1015 Lausanne, Switzerland
[2] Present address: Department of Geological Sciences, 1006 C.C. Little Bldg, University of Michigan, Ann Arbor, MI 48109–1063, USA
[3] Department of Geological Sciences, Campus Box 250, University of Colorado, Boulder, CO 80309-0250, USA

Received April 27, 1992 / Accepted July 6, 1992

Abstract. The oxygen isotope compositions of coesite, sanidine, kyanite, clinopyroxene and garnet were measured in an ultra-high pressure-temperature grospydite from the Roberts Victor kimberlite, South Africa. The $\delta^{18}O$ values (per mil v. SMOW) of each phase and (1 σ) are as follows: coesite, 8.62 (0.31); sanidine, 8.31 (0.02); kyanite, 7.98 (0.08); pyroxene, 7.63 (0.11); garnet, 7.53 (0.03). In situ analyses of the coesite with the laser extraction system are $\delta^{18}O = 9.35$ (0.08), $n = 4$, demonstrating that the coesite is homogeneous. The coesite has partially inverted to polycrystalline quartz and the pyroxene is extensively altered during uplift. The larger scatter for the mineral separate coesite and pyroxene data may be due to partial reequilibration between the decompression-related breakdown products of these two phases. The anomalously high $\delta^{18}O$ value of the grospydite ($\delta^{18}O_{whole\,rock} = 7.7‰$) is consistent with altered oceanic crust as a source rock. Temperature estimates from a linear regression of all the data to three different published calibrations correspond to an equilibrium temperature of 1310 ± 80 °C. The calculated isotopic pressure effect is to lower these estimates by about 40 °C at 40 kb. The estimated temperature based on Al-Si disorder in sanidine is 1200 ± 100 °C and that from Fe-Mg exchange thermometry between garnet and clinopyroxene is 1100 ± 50 °C. Given the large errors associated with thermometry at such high temperatures, it is concluded that the xenolith equilibrated at 1200 ± 100 °C. Pressure estimates are 45 ± 5 kb, based on dilution of the univariant equilibria *albite = jadeite + coesite* and 2 *kyanite* + 3 *diopside = grossular + pyrope* + 2 *coesite*. Zoning in the outer 20 μm of the feldspar from $Ab_{0.8}$ to Ab_{16} indicates rapid decompression to 25 kb or less. The isotopic temperature estimates are the highest ever obtained and combined with the high degree of Al-Si disorder in sanidine require rapid cooling from ultra-high temperatures. It is inferred that the xenolith was sampled at the time of equilibration, providing a point on the upper Cretaceous geotherm in the mantle below South Africa.

Correspondence to: Z.D. Sharp

Introduction

Oxygen isotope thermometry has been applied successfully to a wide range of rock types. The advantages of oxygen isotope thermometry compared to other geothermometric techniques is that it usually requires no pressure correction and can be used over a broad temperature range (e.g., O'Neil 1986). Unfortunately, oxygen isotope thermometry is not suitable for all high temperature rocks. Oxygen isotope fractionations between coexisting phases in many high temperature igneous rocks are relatively insensitive to temperature variations. In slowly cooled metamorphic rocks, significant retrograde oxygen isotope exchange occurs by the process of intracrystalline oxygen diffusion (Bottinga and Javoy 1975; Giletti 1986; Sharp et al. 1988).

The highest temperature estimates from oxygen isotope thermometry are from rapidly cooled igneous rocks (Onuma et al. 1970, Taylor and Epstein 1970; Anderson et al. 1971). Mantle xenoliths are ideal candidates for oxygen isotope thermometry because they meet the "rapidly-cooled" criterion for preserving peak temperatures. Unfortunately, the mafic, undersaturated compositions of nearly all mantle xenoliths are not suited to oxygen isotope thermometry, as the fractionations among common upper mantle phases (pyroxene, garnet, olivine) are very small (O'Neil 1986). In this study, the $\delta^{18}O$ values of mineral separates from an unusual coesite-bearing grospydite were measured in order to estimate temperatures of formation. This mantle nodule is well suited for oxygen isotope thermometry because the fractionations between the coexisting phases (coesite, sanidine, kyanite, garnet and pyroxene) are relatively large, and the rock is thought to have cooled extremely rapidly under anhydrous conditions (Smyth and Hatton 1977).

Pressure-temperature estimates from mantle xenoliths give the most direct indication of the sub-crustal geothermal gradient (e.g., Boyd 1973; Boyd and Nixon 1973; Finnerty and Boyd 1984, 1987). The $\delta^{18}O$ values of mantle samples have been measured (Garlick et al. 1971;

Kyser et al. 1981, 1982; McGregor and Manton 1986; Ongley et al. 1987; Shervais et al. 1988; Caporuscio 1990), but these data have not been used for thermometry except in conjunction with other cation-based thermometers (Kyser et al. 1981). The measured oxygen isotope values of the coesite-sanidine-bearing eclogite (Smyth and Hatton 1977) should provide a check on the cation-based thermometers; any evidence of isotopic disequilibrium may indicate partial reequilibration during relatively slow cooling.

Sample description

A detailed description of the coesite-bearing nodule analyzed in this study (sample SRV 1) has been made by Smyth and Hatton (1977) and is only briefly described here. The sample comes from the Roberts Victor kimberlite near Kimberley, South Africa, and was found by Smyth and Hatton as a 5 kg tabular nodule. The sample consists of an anhedral matrix of clinopyroxene, with subhedral garnet, coesite and sanidine, euhedral kyanite, and very minor pyrrhotite. Approximate abundances of each phase are as follows: pyroxene, 56%; garnet, 28%; kyanite, 9%; coesite, 6%; sanidine, <1%. The matrix pyroxene is extremely aluminous (18 wt.% Al_2O_3) with significant amounts of jadeite (49 mol%) and some substitution of Ca-Tschermaks (6 mol%) and Ca-Eskola (6 mol%) components (Table 1, Fig. 1a). The pyroxene is light green to white in hand sample and is partially altered due to decompression-related exsolution of Ca-Tschermaks component (Smyth and Hatton 1977) (Fig. 1a). The garnets have an average composition of $Gr_{47}Py_{28}Al_{25}$ (Table 1), are up to 5 mm in diameter and show almost no alteration. Colorless coesite grains are up to 3 mm in diameter, with ubiquitous alteration rims of polycrystalline quartz (Fig. 1b, c) and have >99.9 wt.% SiO_2. The nearly colorless sani-

Table 1. Microprobe analyses of selected phases in sample SRV-1

	Garnet[a]	Omphacite[b]	Sanidine[c]	
			(Core)	(Rim)
SiO_2	39.84	56.13	64.06	64.36
TiO_2[d]	0.17	0.07	0.00	0.00
Al_2O_3	23.20	17.95	18.83	19.08
FeO[e]	12.19	1.84	0.01	0.02
MgO	7.64	5.89	0.00	0.00
MnO[d]	0.29	0.00	0.00	0.00
CaO	17.82	11.15	0.01	0.04
K_2O	0.01	0.18	17.37	14.60
Na_2O	0.07	7.33	0.10	2.00
Sum	101.22	100.53	100.38	100.11
Si	2.941	1.940	2.949	2.940
Ti	0.009	0.002	0.000	0.000
Al	2.018	0.731	1.021	1.028
Fe	0.752	0.053	0.000	0.001
Mg	0.841	0.304	0.000	0.000
Mn	0.018	0.000	0.000	0.000
Ca	1.409	0.413	0.000	0.002
K	0.001	0.008	1.020	0.851
Na	0.010	0.491	0.009	0.177
vacancy	0	0.058	0	0

[a] Normalized to 8 cations; [b] normalized to 6 oxygens for vacancy calculation; [c] normalized to 5 cations; [d] data for this element from Smyth and Hatton (1977); [e] all iron assumed as ferrous

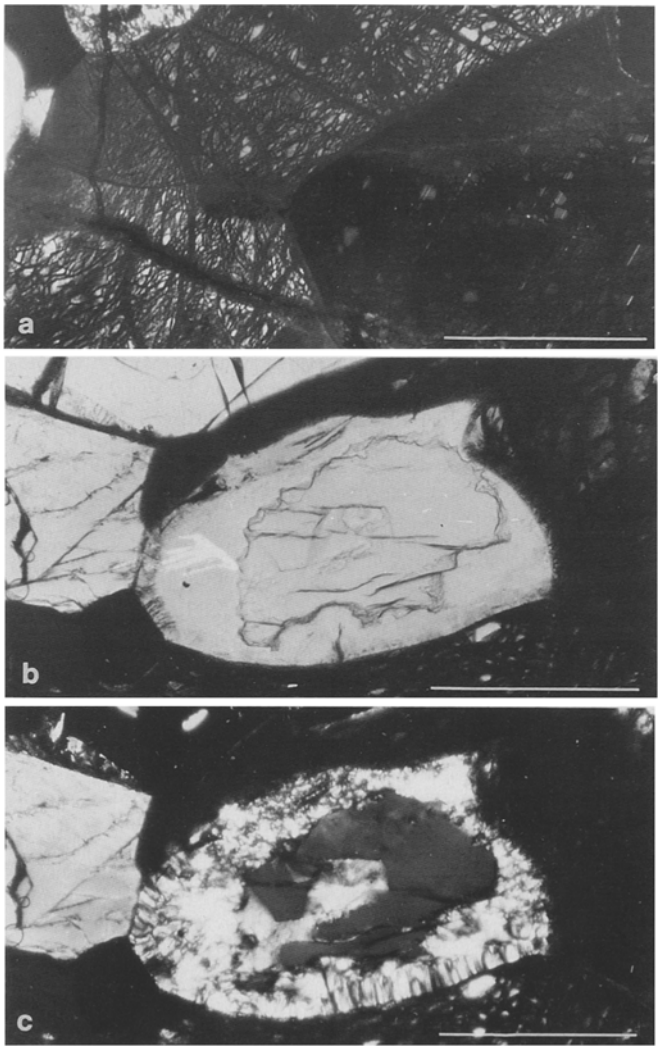

Fig. 1. a Photomicrograph of pyroxene showing the decompression-related breakdown of the high-pressure Ca-Tschermak and Ca-Eskola components. Scale bar = 300 μm. **b–c** Coesite with ubiquitous inversion rim to quartz in plane-polarized (**b**) and cross-polarized light (**c**). Other minerals: pyroxene (groundmass), kyanite (*left*), garnet (*top-left*). Scale bar = 300 μm

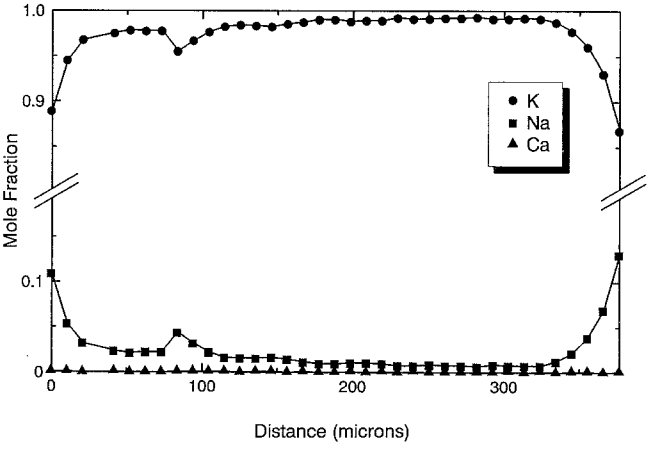

Fig. 2. Zoning profile in sanidine measured with the electron microprobe

dine is very highly disordered (Scambos et al. 1987); it is chemically zoned with a core composition $Or_{99}Ab_1$ and a rim composition in the outer 20 μm of $Or_{83}Ab_{17}$ (Table 1; Fig. 2). Kyanite grains are up to 3 mm across, light blue in color with no alteration, and are nearly pure Al_2SiO_5. Previous pressure-temperature estimates for the nodule are 48–50 kb and 1050–1125 °C (Wohletz and Smyth 1984; McCormick and Smyth 1986).

Analytical methods

Oxygen isotope compositions were determined with the laser based extraction method of Sharp (1990) on mineral separates and by in situ measurements on coesite. For mineral separates, a small sample was crushed, ultrasonically cleaned in distilled water, and sieved to between 180–250 μm mesh. Preliminary separation of the samples was made with heavy liquids. The sample was treated with methylene iodide ($d = 3.31$–3.32) to separate garnet and kyanite from the coesite, sanidine and pyroxene. Sanidine was further concentrated by floating in bromoform ($d = 2.814$–2.818). The coesite- and sanidine-concentrates were passed through a magnetic separator; coesite and sanidine were then handpicked from their respective concentrates and treated for 30 s in hydrofluoric acid to weakly etch the sanidine. This allowed for the coesite and sanidine to be distinguished optically. A final handpicking of each concentrate resulted in a purity for both the sanidine and coesite separates that approached 100%. Pure garnet and kyanite separates were obtained by simple handpicking of the coarse-grained heavy concentrate. The purity of all concentrates was checked under crossed polars in a petrographic microscope.

The in situ analyses were made on a 200 μm thick, doubly polished plate (Fig. 3). Coesite grains were first identified with EDS spectroscopy on an SEM at the University of Lausanne before laser analysis. A detailed description of the laser extraction technique is given by Sharp (1990, 1992) and is only briefly described here. Mineral separate analyses were made on about 1 mg of material. Fifteen to eighteen samples were loaded simultaneously on a nickel sample holder. A minimum of three laboratory quartz standards (relative to NBS-28 = 9.5‰) were analyzed in every block of 15–18 samples; all phases were analyzed at least twice. A 20 W CO_2 laser was used for heating, with a BrF_5 oxidizing reagent at 0.1 bar. All mineral phases could be reacted to 100% completion with the laser extraction technique. The in situ analyses on coesite were made by a series of pulses of the focused laser at 6 W power; each pulse duration was 50–80 ms. Pulsing continued until a hole was bored through the thin plate. The gas was converted to CO_2 via combustion of a heated graphite rod with a platinum catalyst and introduced directly into the mass spectrometer.

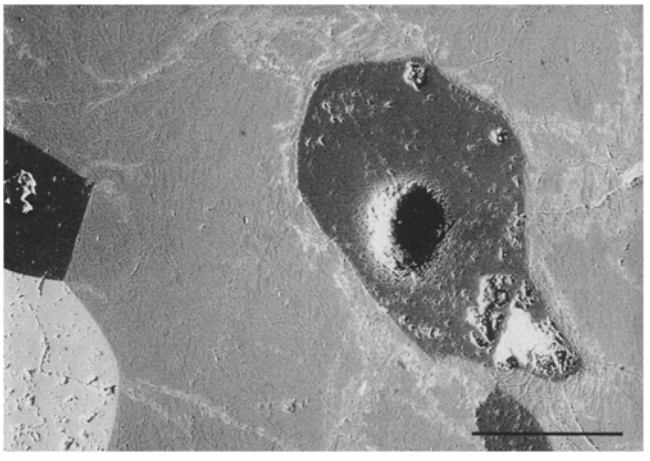

Fig. 3. Backscatter electron image of a 200 μm thick plate of the coesite-bearing grospydite. The hole in the coesite grain (dark grey) constitutes a single oxygen isotope analysis with the in situ laser method (Sharp 1990). Scale bar = 300 μm. Light grey matrix, pyroxene; white grain, garnet; black grain, kyanite

Major element analyses were made with a Cameca SX50 microprobe at the University of Lausanne. Analyses were made with a tightly focused beam rastered over a 25 μm^2 area at 15 kV and 10 nA sample current. The analytical standards jadeite, diopside, and orthoclase were used for calibration. The PAP correction program supplied by Cameca was used for data reduction. Mineral normalizations were made with the aid of the program MINFILE (Afifi and Essene 1988).

Results

The $\delta^{18}O$ values of all mineral separates and in situ analyses are given in Tables 2 and 3. The standard deviations for the data from mineral separates of garnet, kya-

Table 2. Oxygen isotope ratios for all mineral separates

Mineral	Run number	$\delta^{18}O$ (SMOW)	Sample size (mg)
Garnet	S058-7	7.58	1.46
	S058-8	7.49	0.90
	S074-5	7.52	1.52
	S097-5	7.52	1.75
	S097-6	7.56	1.83
	Avg. (1 σ)	7.53 (0.03)	
Pyroxene	S097-7	7.71	1.78
	S097-8	7.48	1.30
	S098-6	7.55	1.82
	S098-7	7.76	1.28
	Avg. (1 σ)	7.63 (0.11)	
Kyanite	S058-9	7.89	1.38
	S058-10	8.11	0.88
	S074-6	7.99	1.03
	S097-9	7.99	1.46
	S097-10	7.90	1.80
	Avg. (1 σ)	7.98 (0.08)	
Coesite	S097-3	14.38[a]	0.60
	S097-4	8.36	0.52
	S098-4	9.05	0.80
	S099-3	8.77	1.02
	S099-4	8.28	0.76
	Avg- (1 σ)	8.62 (0.31)	
Sanidine	S098-5	8.33	1.39
	S099-5	8.28	1.03
	Avg. (1 σ)	8.31 (0.02)	
Whole rock		7.7[b]	

[a] Excluded from average; [b] calculated based on mineral modes of Smyth and Hatton (1977)

Table 3. Oxygen isotope values of in situ analyses of coesite. Each analysis is a single 200 μm diameter hole

Run number	$\delta^{18}O$ (SMOW)	μmoles CO_2
S096-2	9.38	0.9
S096-4	9.44	0.8
S096-5	9.34	2.0
S096-6	9.22	1.6
Avg (1 σ)	9.35 (0.08)	

nite and sanidine are all very small, indicating a high degree of homogeneity. The pyroxene data have only a slightly larger range in $\delta^{18}O$ values, which may be related to the extensive alteration and/or retrograde isotopic exchange. The $\delta^{18}O$ values of the coesite have the largest spread. The $\delta^{18}O$ values range from 8.28–9.05‰, excluding an anomalous value of 14.38‰. This large range in $\delta^{18}O$ may be due to either (1) real sample heterogeneities, (2) partial reequilibration of the coesite during retrogression or (3) contamination by other phases. The degree of sample contamination for coesite can be assessed visually with the laser extraction system. The fluorination products of SiO_2 are all gases (Br_2, BrF_3, SiF_4); any residual solid fluoride in the sample chamber indicates sample contamination. In all cases, very minor or no residues were observed. Assuming an unreasonably high sample contamination of 20% by the isotopically lightest phase in the rock, the shift in the $\delta^{18}O$ would still be <0.2‰. The variations in the $\delta^{18}O$ of coesite, therefore, cannot be explained exclusively by contamination.

Potential isotopic heterogeneity of the coesite was assessed by making in situ analyses of coesite. The high spatial resolution (~ 200 μm) of the in situ technique (Fig. 3) allows for analyses to be made on pure, uncontaminated material. All in situ $\delta^{18}O$ values are 9.35 ± 0.08‰ (Table 3), demonstrating that the coesite is isotopically homogeneous. The in situ $\delta^{18}O$ values are slightly higher than those obtained on mineral separates. This ^{18}O enrichment may be due to an isotopic shift associated with the in situ method for coesite. There is no shift associated with in situ analyses of quartz plates (Sharp 1992; Kirschner et al. 1992), but other refractory phases, such as garnet, do exhibit an isotopic shift (Sharp 1992). In contrast to the in situ data, no isotopic shift has been observed on mineral separate data with the laser extraction system (Sharp 1990, 1992); therefore, the mineral separate data are accepted as the true isotopic composition. The in situ data are used to demonstrate that the coesite is isotopically homogeneous.

A possible explanation for the large range in measured coesite $\delta^{18}O$ values is retrograde exchange with the host pyroxene. The coesite has a ubiquitous inversion rim to polycrystalline quartz (Fig. 1 b, c), and the pyroxene is partially altered, presumably due to the instability of the Ca-Eskola, Ca-Tschermaks and jadeite components during decompression (Fig. 1 a). If oxygen isotope exchange between the inverting coesite and the decomposing pyroxene occurred during decompression, there could be a significant shift in the $\delta^{18}O$ values of the SiO_2 polymorphs. Even slight retrograde deformation can cause significant isotopic exchange (e.g., Sharp et al. 1988). If 20% of the coesite inverted to quartz and exchanged with the surrounding pyroxene at temperatures of about 700 °C, the $\delta^{18}O$ of the quartz would be 1.8‰ higher than the coesite, and the sum of the two would be about 0.4‰ higher than the unaltered coesite. An isotopic fractionation between the two silica polymorphs is predicted based on electrostatic site potential calculations for oxygen (Smyth 1989). At 1000 °C, the calculated fractionation between quartz and coesite is 0.2‰, based on the data of Smyth (1989) and the equation of Smyth and Clayton (1988). This difference will be as large as 1‰ at 40 kb (see following discussion). Preferential analysis of either the polycrystalline quartz or the coesite will lead to a large scatter in the isotopic data for the SiO_2 polymorph.

There are several lines of evidence supporting the hypothesis for retrograde exchange. First, the pyroxene has a larger standard deviation than the unaltered phases garnet, sanidine and kyanite. Partial exchange with the inverting coesite would explain this small degreee of heterogeneity. Secondly, analyses of the $\delta^{18}O$ of the coesite in the same sample by Jeffrey Deen measured in the laboratory of R.O. Rye, U S G S, Denver with the conventional fluorination technique (Clayton and Mayeda 1963) are in the range 9.5 to 10.2‰. Very low yields were obtained due to the extreme difficulty of fluorinating coesite. The high $\delta^{18}O$ values obtained conventionally probably reflect a preferential reaction of the ^{18}O-enriched polycrystalline quartz as compared to the more refractory coesite.

Oxygen isotope thermometry

Temperature estimates based on the isotopic fractionations between all phases are given in Table 4 and shown graphically in Fig. 4 a–d. Four calibrations were used: (1) Bottinga and Javoy (1975); (2) the incremental method of Richter and Hoernes (1988) with the modified data set of Hoffbauer et al. (1992); (3) Smyth and Clayton (1988) using the oxygen site potentials of Smyth (1989); and (4) experimentally determined calibrations of Lichtenstein and Hoernes (1992) for quartz-garnet and Chiba et al. (1989) for all other phases. The fractionation factor for albite was used in place of sanidine for the temperature estimates with the fractionation factors of Bottinga and Javoy (1975) and Chiba et al. (1989). This substitution is justified as there is no oxygen isotope fractionation associated with K-Na exchange in feldspar (O'Neil and Taylor 1967; T Chacko, personal communication 1992). A correction for the jadeite component in clinopyroxene based on the temperature coefficient of fractionation a_{Di-Jd} relationship of Matthews et al. (1983) was made for the temperature estimates made with the fractionation factors of Bottinga and Javoy (1975) and Chiba et al. (1989). The fractionation factors with the technique of Hoffbauer et al. (1992) were kindly calculated by Dr. R. Hoffbauer for the exact mineral compositions given in Table 1. A fractionation factor intermediate to diopside and jadeite was used for the Smyth and Clayton calibration.

Oxygen isotope fractionations between any two phases are related by the equation:

$$\Delta_{i-j} = a_{ij} \times 10^6/(T^2) + b_{ij} \quad (T \text{ in K}) \qquad (1)$$

where Δ_{i-j} is the difference in the isotopic compositions of phases i and j, a_{ij} is the temperature coefficient of the fractionation equation for the mineral pair $i-j$ and b_{ij} is the isotopic fractionation between mineral pair $i-j$

Table 4. Oxygen isotope thermometric estimates (°C). Abbreviations: Coe, coesite; Sd, sanidine; Ky, kyanite; Di, diopside; Om, omphacite; Gt, garnet

	Sd	Ky	Di	Om	Gt
Experimental calibrations[a, b, c]					
Coe	1470	1370	1400	1240	1340
Sd		1280	1360	1120	1290
Ky			1430	950	1290
Di					620
Om					2140
Bottinga and Javoy (1975)[a, b]					
Coe	1500	–	1370	1210	1350
Sd		–	1310	1060	1290
Ky			–	–	–
Di					1180
Om					2390
Smyth and Clayton (1988)[d]					
Coe	1170	1550	1280	1150	1330
Sd		1850	1330	1150	1390
Ky			580	∞	950
Di					1780
Om					2580
Hoffbauer et al. (1992)[a, d]					
Coe	1520	1840	1370	1230	1450
Sd		2100	1300	1080	1430
Ky			∞	∞	650
Di					2000
Om					2940

[a] The fractionation factor for quartz was used in place of coesite. [b] The fractionation factor for albite was used in place of sanidine; the fractionation factor for omphacite was assumed to be midway between that of diopside and jadeite based on the diopside-jadeite calibration of Matthews et al. (1983). [c] All fractionation factors from Chiba et al. (1989) except quartz-garnet from Lichtenstein and Hoernes (1992), and kyanite (empirical) from this study. [d] Fractionation factor for garnet corrected for solid-solution

at infinite temperature (Clayton and Epstein 1961; Bottinga and Javoy 1973). For the phases and calibrations considered in this study, $b=0$, and will be left out of the following equations. A temperature estimate for all coexisting minerals in a rock can be made with the isotherm method of Javoy et al. (1970) by rearranging Eq. 1 to a simple linear form

$$\Delta_{i-k}=a_{ik}\times 10^6/(T^2)(T \text{ in K}), \quad (2)$$

where all phases i are treated in terms of one of the phase k (the choice of k is arbitrary), and $b=0$. All data will plot on a Δ_{i-j} versus a_{i-j} diagram as a straight line with a slope of T^{-2} if all phases are in equilibrium. Equation 2 requires the assumptions that the phase i has a single value and the statistical best fit of Δ_{i-j} versus a_{i-j} must pass through zero (i.e., Δ_{k-k} and $a_{k-k}=0$). Equation 2 can be generalized to incorporate every measurement of each phase so that temperatures can be calculated with a linear best fit to *all* of the measurements by the following equation:

$$\delta_{ij}=a_{jk}\times 10^6/(T^2)+C\,(T \text{ in K}) \quad (3)$$

Table 5. Empirical estimation of the a(Qz-Ky) and a(Ky-Gt) temperature coefficient from published data on quartz – kyanite – garnet triplets

Reference	(1)	(2)	(2)	(3)	(4)	(4)
δ^{18}O (Quartz)	0.00	8.70	8.40	14.00	9.41	7.83
δ^{18}O (Kyanite)	−4.70	6.40	6.10	10.90	7.71	6.76
δ^{18}O (Garnet)	–	5.10	5.10	9.50	5.17	4.79
T(Qz-Gt)	430[a]	615	650	520	545	690
a(Qz-Ky)	2.32	1.81	1.97	1.95	1.13	1.00
a(Ky-Gt)	0.37	1.02	0.86	0.88	1.70	1.83

Reference	(5)	(5)	(5)	(5)	(5)	(5)
δ^{18}O (Quartz)	23.05	10.60	10.35	–	18.55	14.00
δ^{18}O (Kyanite)	18.50	8.00	4.70	7.15	15.50	10.15
δ^{18}O (Garnet)	18.60	6.10	6.00	5.55	14.60	10.15
T(Qz-Gt)	525	520	535	670[b]	575	585
a(Qz-Ky)	2.89	1.64	3.68	1.42	2.19	2.83
a(Ky-Gt)	−0.06	1.19	−0.85	1.41	0.64	0.00

[a] Equilibration temperature determined from quartz-muscovite fractionation. [b] Equilibration temperature determined from garnet-ilmenite fractionation. References: (1) Taylor et al. 1963; (2) Garlick and Epstein 1965; (3) Hoernes and Hoffer 1979; (4) G. Frueh Green, ETH, Zurich, unpublished data; (5) Hoernes and Friedrichsen 1980

where δ_{ij} is the ith measurement of phase j, a_{jk} is the temperature constant of phase j relative to a reference mineral k (garnet was used in this study, although the choice of a reference mineral is arbitrary) and C is a constant. A least squares fit of all δ_{ij} measurements with respect to the corresponding a_{jk} constants yields a slope equal to T^{-2} with a y intercept equal to C. Equation 3 is more general than Eq. 2. Equation 2 forces the y intercept to be zero, while Eq. 3 eliminates this constraint. Graphical representations of Eq. 3 and temperature estimates based on the four different isotope calibrations are shown in Fig. 4a–d.

Temperature estimates and regression uncertainties using is method are as follows: Bottinga and Javoy (1975), 1320 (±90) °C; experimental calibrations, 1310 (±80) °C; Smyth and Clayton (1988), 1310 (±90) °C; Hoffbauer et al. (1992), 1400 (±50) °C. The kyanite data were excluded from all regressions.

Fractionation factors involving kyanite have not been estimated by Bottinga and Javoy (1975) or measured experimentally, but Smyth (1989) and Hoffbauer et al. (1992) provide kyanite fractionation data. In these two calibrations, the data for kyanite lie well off the isotherm defined by the other phases (Fig. 4c, d). The temperature coefficient of fractionation a for kyanite (relative to either quartz or garnet) was determined empirically in this study using published δ^{18}O values of quartz-kyanite-garnet assemblages (Table 5). Equilibration temperatures for these quartz-kyanite-garnet triplets were determined from the measured Δ_{gt-qz} and the calibration of Lichtenstein and Hoernes (1992). The garnet-kyanite or quartz-kyanite temperature coefficient of fractionation a could then be calculated with Eq. 1.

The average a_{ky-gt} in Table 5 is 1.1±0.5 (excluding negative values). The large standard deviation of this

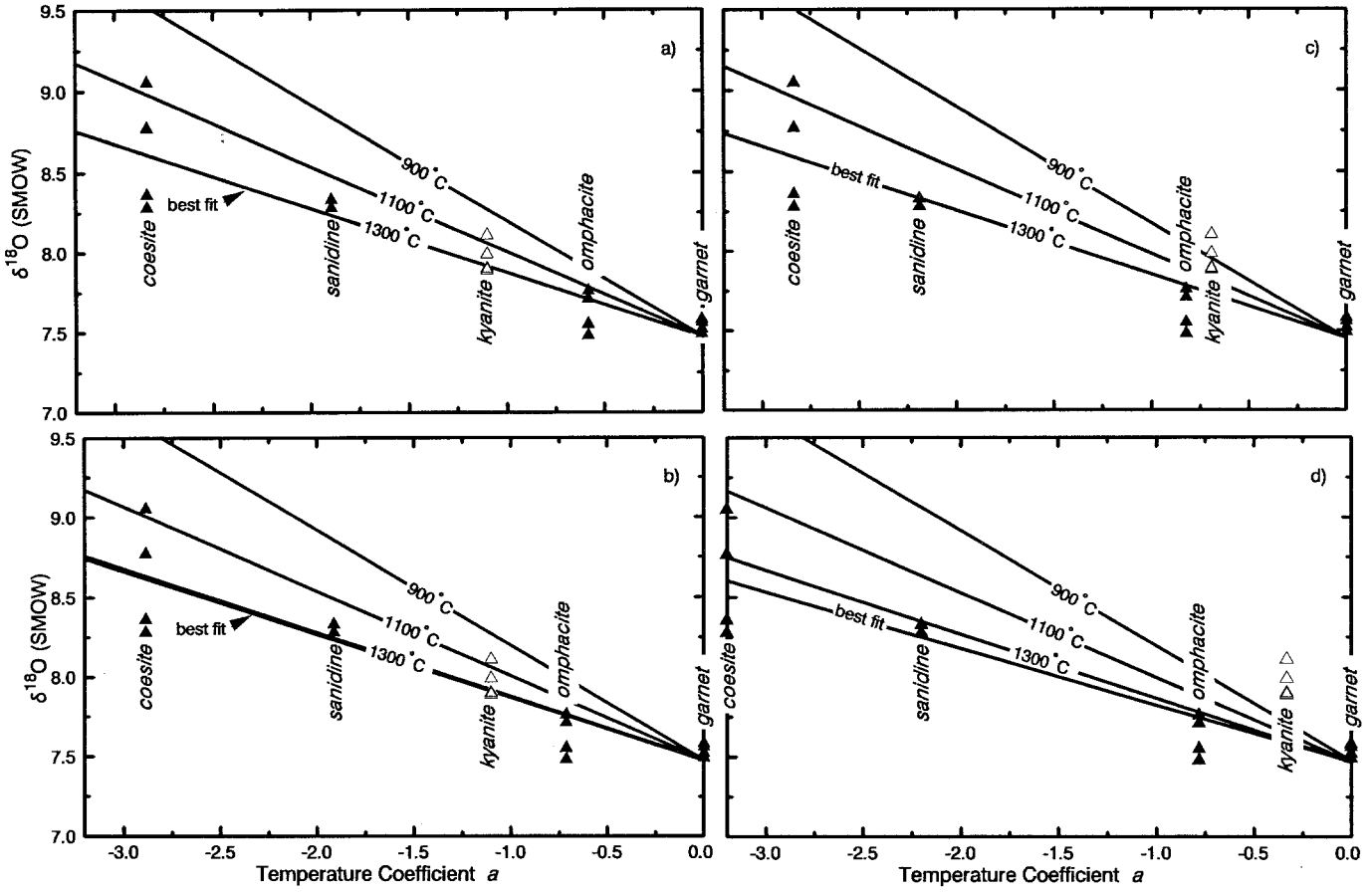

Fig. 4a–d. Graphical presentation of temperature estimates by Eq. 3. The isotopic composition ($\delta^{18}O$ $value_{SMOW}$) of every measurement for each mineral is plotted against the temperature coefficient a (from Eq. 1) for that mineral relative to garnet. The slope of the best fit line to all the data is related to the temperature by Eq. 3. **a** From experimental calibrations (Chiba et al. 1989; Lichtenstein and Hoernes 1992); **b** Bottinga and Javoy (1975); **c** Smyth and Clayton (1988); **d** Hoffbauer et al. (1992)

value is almost certainly due to analytical errors, because kyanite is so difficult to fluorinate with conventional extraction techniques (in contrast, kyanite is easily fluorinated with the high-temperature laser extraction method). The temperature estimate for the grospydite SRV 1 using the value 1.1 for temperature coefficient a_{ky-gt} is 1290 °C, in agreement with other fractionations, although the uncertainties in the estimate for the temperature coefficient a may make this agreement fortuitous.

The polymorphic transition quartz-coesite may impose an additional complication to the oxygen isotope temperature estimates of the coesite-bearing grospydite. In the four calibrations applied in this study, only that of Smyth and Clayton (1988) with the electrostatic site potential data for coesite of Smyth (1989) provides fractionation factors in place of coesite. In all the others, quartz was used in place of coesite. The difference in the average site potentials for quartz and coesite is 0.45 V, corresponding to an $a_{qz\text{-}coe}$ of 0.35 and a Δ_{qz-coe} of 0.14 at 1300 °C. Although this difference is small, an $a_{coe-garn}$ value of 2.48 is obtained when the $a_{qz\text{-}coe}$ value of 0.35 is subtracted from the experimentally determined $a_{qz-garn}$ value of 2.83. Application of this $a_{coe-garn}$ coefficient will result in temperature estimates that are 100 °C lower than those based on the experimental quartz-garnet fractionation. Preliminary measurements of Δ_{qz-coe} by Sharp and P. Ulmer (ETH, Zurich) following the procedure of Clayton et al. (1989) do not support the theoretical fractionation indicated by the electrostatic data. In addition, no quartz-coesite fractionation is predicted by the increment method (Hoffbauer et al. 1992). It is therefore reasonable to use the quartz fractionation factors for coesite.

Temperature estimates from Al-Si disorder in feldspar

The very high temperature estimates from the stable isotope data are supported by the extraordinarily high degree of Al-Si disorder in the sanidine (Scambos et al. 1987). The sanidine exceeds the upper limits of Al-Si disorder that have been measured on one atmosphere, experimentally disordered samples. The degree of Al-Si disorder in feldspars increases with temperature, so that an estimate of disorder in a crystal defines a minimum temperature of equilibration. The unit cell parameters of Scambos et al. (1987) are $a=8.595(3)$ Å, $b=13.028(5)$ Å and $c=7.175(2)$ Å. A measure of the Al-Si disorder can be calculated from the relation (Hovis 1986)

$$Z=-138.575+19.3153\,c_k \quad (4)$$

where $c_k = c_{obs} + 0.0381\ (1 - N_{Or})$ and the degree of disorder Z is defined as $2[N_{A1(T1)} - N_{A1(T2)}]$. The disorder term Z is 0.02 by this technique. Alternatively, Z may be estimated from the T-O distance technique of Kroll and Ribbe (1983) with the structure refinement of Scambos et al. (1987); the Z from this method is 0.06. Temperature estimates, corrected for pressure, are made from the following relation of Hovis (1974):

$$T(\mathrm{K}) = \frac{\Delta E^0 + P\Delta V^0}{\Delta S^0 - 2R\ \mathrm{ath}\,[4Z/(3+Z^2)]} \tag{5}$$

where

$$\mathrm{ath}\,(x) = 0.5 \ln [(1+x)/(1-x)]. \tag{6}$$

In Eq. 5, $\Delta E^0 = -22200$ J/mol, $\Delta S^0 = -15.5$ J/deg·mol, $\Delta V^0 = -0.054$ J/bar·mol; P in bar. Temperature estimates from Eq. 5 for $Z = 0.02$ and $Z = 0.06$ are 1220 and 1140 °C at 30 kb and 1310 and 1220 °C at 55 kb, respectively.

Geothermobarometric estimates from mineral equilibria

Various univariant equilibria involving the phases garnet, clinopyroxene, feldspar, coesite and kyanite are applicable to the sample SRV-1. The equilibria considered in this study are the following:

$$\underset{\text{albite}}{NaAlSi_3O_8} = \underset{\text{jadeite}}{NaAlSi_2O_6} + \underset{\text{coesite}}{SiO_2} \tag{7}$$

$$\underset{\text{almandine}}{Fe_3Al_2Si_3O_{12}} + 3\underset{\text{diopside}}{CaMgSi_2O_6} = \underset{\text{pyrope}}{Mg_3Al_2Si_3O_{12}} + 3\underset{\text{hedenbergite}}{CaFeSi_2O_6} \tag{8}$$

$$\underset{\text{kyanite}}{2Al_2SiO_5} + 3\underset{\text{diopside}}{CaMgSi_2O_6} = \underset{\text{coesite}}{2SiO_2} + \underset{\text{pyrope}}{Mg_3Al_2Si_3O_{12}} + \underset{\text{grossular}}{Ca_3Al_2Si_3O_{12}} \tag{9}$$

$$\underset{\text{kyanite}}{2Al_2SiO_5} + 3\underset{\text{diopside}}{CaMgSi_2O_6} + 2\underset{\text{jadeite}}{NaAlSi_2O_6} = 2\underset{\text{albite}}{NaAlSi_3O_8} + \underset{\text{pyrope}}{Mg_3Al_2Si_3O_{12}} + \underset{\text{grossular}}{Ca_3Al_2Si_3O_{12}}. \tag{10}$$

In order to use these equilibria for accurate thermobarometric estimates, it is necessary to adjust the equilibrium curves of each reaction for the solid solutions present in the phases clinopyroxene, garnet and feldspar. Activity models for each of these phases are essential for accurate pressure-temperature estimates.

Activity models

The activity of $NaAlSi_3O_8$ in sanidine was determined with the ternary feldspar model of Fuhrman and Lindsley (1988) with the updated excess volume terms (W_v) of Lindsley and Nekvasil (1989). The pressure effect on the activity-composition ($a-X$) relations is very large in the pressure range experienced by the grospydites (Fig. 5). The $NaAlSi_3O_8$ activity at $X(NaAlSi_3O_8) = 0.01$ increases from 0.01 at 1 bar to 0.09 at 50 kb (1200 °C). The validity of this large pressure correction was evaluated by plotting the ($a-X$) relation for alkali feldspar at the critical point of the solvus from 0.001 – 40 kb (Thompson and Waldbaum 1969) (Fig. 6). A horizontal slope in the $a-X$ relations at any pressure and temperature indicates that the solvus is reached. At all $P-T$ values plotted in Fig. 6, a horizontal slope occurs, in agreement with the solvus data of Thompson and Waldbaum (1969). This substantiates the large pressure effect indicated by the W_v of Lindsley and Nekvasil (1989),

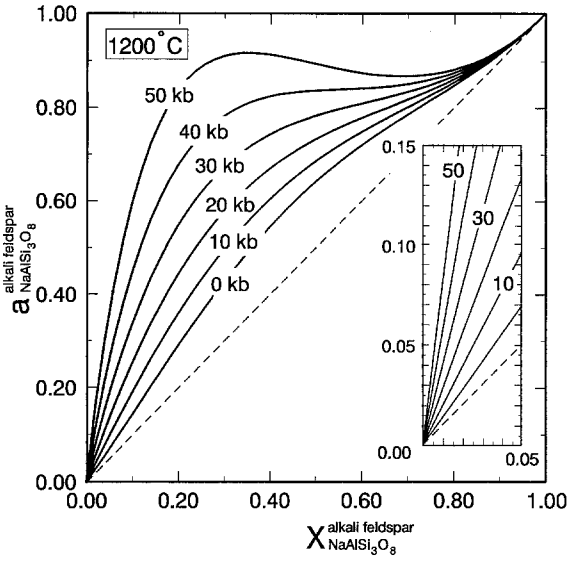

Fig. 5. Activity-composition relation for activity of $NaAlSi_3O_8$ in sanidine for various pressures with parameters of Lindsley and Nekvasil (1989). In the dilute range considered in this study (*inner box*) pressure has a strong effect on the activity-composition relations

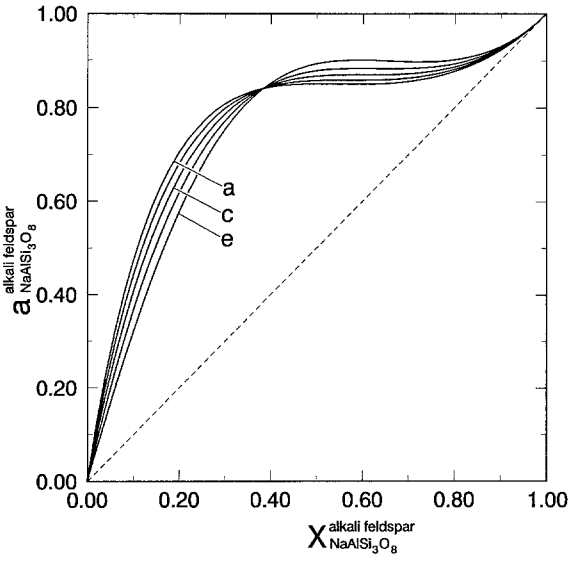

Fig. 6. Activity-composition relation for $NaAlSi_3O_8$ in sanidine at the critical solvus conditions defined by Thompson and Waldbaum (1969). The *horizontal line* in each curve satisfies the thermodynamic conditions that a solvus exists at that given pressure and temperature. P–T as follows (P in kb; T in °C): *a* – 0.001, 650; *b* – 10, 780; *c* – 20, 910; *d* – 30, 1020; *e* – 40, 1170

although extrapolations to 40 kb should theoretically include a W term for compressibility (Lindsley, personal communication 1992).

Garnet activities were estimated from the quaternary mixing model of Berman (1990). The calculated activities of $Mg_3Al_2Si_3O_{12}$, $Fe_3Al_2Si_3O_{12}$ and $Ca_3Al_2Si_3O_{12}$ in garnet based on earlier $a-X$ models (e.g., Ganguly and Saxena 1984; Anovitz and Essene 1987) are more ideal and yield slightly lower pressures and temperatures based on the calculated equilibria of reactions 8–10. Substitution of a Wohl ternary interaction parameter $C_{123} = -66.4$ kJ/mol (Ganguly and Saxena 1984) in place of the $C_{123}=0$ assumed by Berman (1990) will shift the location of reactions 8–10 less than 20 °C and 2 kb.

The clinopyroxene composition in sample SRV-1 (Table 1) can be approximated by the major components jadeite ($NaAlSi_2O_6$) and diopside ($CaMgSi_2O_6$), with minor hedenbergite ($CaFeSi_2O_6$), Ca-Eskola molecule ($Ca_{0.5}\square_{0.5}AlSi_2O_6$), and Ca-Tschermaks component ($CaAl_2SiO_6$). The quaternary system jadeite-diopside-hedenbergite-Ca-Eskola adequately describes the pyroxene, but $a-X$ relations involving Ca-Eskola are limited to the Ca-Eskola – Ca-Tschermaks join (Gasparik 1984), so that quaternary mixing terms in the above system could not be calculated. The activities of $NaAlSi_2O_6$, $CaMgSi_2O_6$, and $CaFeSi_2O_6$ in clinopyroxene (cpx) were calculated using the jadeite-diopside-hedenbergite ternary of Anovitz (1991) based on the jadeite-diopside binary relations of Cohen (1986) and assuming ideal mixing between diopside and hedenbergite. The activity coefficient (γ) for each end-member was calculated at the pressure and temperature of interest by normalizing $X_{\text{jadeite}}+X_{\text{diopside}}+X_{\text{hedenbergite}}=1$. The activities of each component were then estimated as follows: $a(NaAlSi_2O_6$ in cpx$)=(X_{Na})\cdot(X_{Al})\cdot(X_{Si})^2\cdot(\gamma_{Jd})$, $a(CaMgSi_2O_6$ in cpx$)=(X_{Ca})\cdot(X_{Mg})\cdot(X_{Si})^2\cdot(\gamma_{Di})$ and $a(CaFeSi_2O_6$ in cpx$)=(X_{Ca})\cdot(X_{Fe})\cdot(X_{Si})^2\cdot(\gamma_{Di})$ where all cations (including vacancies) are normalized to 4.

Pressure-temperature estimates

The P-T locations of reactions 7–10 were calculated with the computer program THERMOCALC (Powell and Holland 1988) for the thermodynamic data set of Holland and Powell (1990) corrected for reduced activities outlined already. Pressure estimates from the intersection of reactions 7, 9 and 10 are 44 kb at 1110 °C (Fig. 7). The feldspar is zoned in the outer 50 microns due to new growth of more sodic feldspar by the net-transfer reactions 7 and 10 (Fig. 2) and is consistent with pressures of 25–30 kb (Fig. 7).

The garnet-clinopyroxene exchange reaction 8 is the only reaction considered that is strongly temperature sensitive. The calculated equilibria for reaction 8 corrected for solid solution occurs at 1000 °C at 43 kb, far lower than estimates from either the isotopic data or Al-Si disorder data from sanidine. The calculated $P-T$ position of this reaction is very sensitive to small changes in the free energy of the end-member phases. Small uncertainties in the thermodynamic data or $a-X$ relations for any of the phases in reaction 8 can dramatically shift the calculated $P-T$ location of this reaction. More reliable temperature estimates can be obtained with experimental calibrations of the Fe-Mg garnet-clinopyroxene exchange thermometer (e.g., Råheim and Green 1974; Ellis and Green 1979; Pattison and Newton 1989; see references in Fonarev et al. 1991). Temperature estimates with the Ellis and Green calibration are 1120 °C, in excellent agreement with the invariant point of reactions 7, 9 and 10, but lower than the estimates from either oxygen isotope thermometry or Al-Si disorder in sanidine. Temperature estimates based on Powell (1985) and Krogh (1988) are in agreement with those from Ellis and Green (1979), while the calibration of Pattison and Newton (1989) yields far lower temperatures. Pattison and Newton (1989) state that their calibration "does not address the problem of K_D versus T in eclogites with omphacite of jadeite contents approaching 50%". In a comparison of the different thermometers, Fonarev et al. (1991) suggesting using the Ellis and Green calibration for samples above 1200 °C. Overall, the pressure, temperature and composition range of the Ellis and Green experiments more closely match the xenolith composition and metamorphic conditions than those of Pattison and Newton.

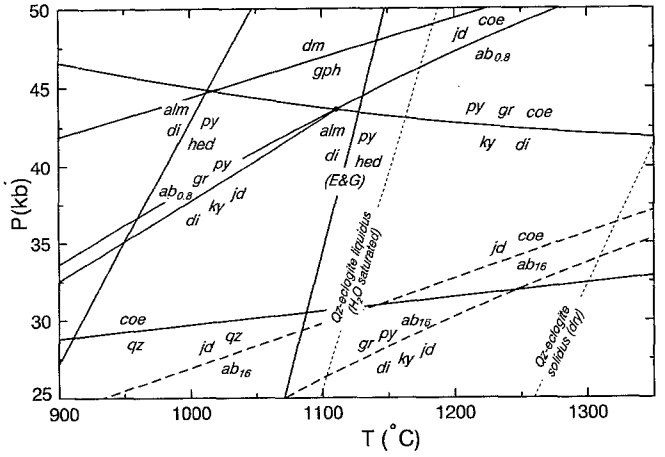

Fig. 7. Pressure-temperature diagram of selected equilibria. The equilibria coesite = quartz from Bohlen and Boettcher (1982); graphite = diamond from Kennedy and Kennedy (1976). Melting relations from Green and Ringwood (1967), Ito and Kennedy (1971) and Lambert and Wyllie (1972). The Fe-Mg garnet-clinopyroxene exchange reaction (*E&G*) was calculated with the formula from Ellis and Green (1979). All other equilibria calculated with the computer program THERMOCALC (Powell and Holland 1988) and the thermodynamic data set of Holland and Powell (1990) corrected for solid solution. Abbreviations: $ab_{0.8}$, albite ($X_{\text{albite}}=0.008$); ab_{16}, albite ($X_{\text{albite}}=0.16$); *alm*, almandine; *coe*, coesite; *di*, diopside; *dm*, diamond; *gph*, graphite; *gr*, grossular; *hed*, hedenbergite; *jd*, jadeite; *ky*, kyanite; *py*, pyrope

Discussion

Pressure estimates from the reaction 7, 9 and 10 are greater than 40 kb. The effect of pressure on oxygen isotope thermometry is thought to be insignificant for crustal pressures (Hoering 1961; Clayton et al. 1974) and

is routinely ignored. There have not been, however, any previous oxygen isotope thermometric studies of samples equilibrated at such high pressures. It is therefore worthwhile to estimate any potential pressure contribution to the measured oxygen isotope fractionations in sample SRV-1.

Effect of pressure on oxygen isotope fractionations

Clayton et al. (1974) and Clayton (1981) estimated that the $\Delta V_{\text{reaction}}$ for a typical solid-solid reaction is on the order of 25×10^{-3} J/mole·kb. A rough estimate of the effect of pressure on a typical oxygen isotope exchange reaction can be estimated from the relationship

$$\frac{d(1000 \ln K)}{dP} = 1000 \frac{P\Delta V}{RT} \quad (11)$$

At temperatures of 1100 °C and 40 kb, the isotopic shift due to pressure will be less than 0.1‰, assuming a $\Delta V_{\text{reaction}}$ of 25×10^{-3} J/mole·kb. Such a pressure effect is nearly insignificant when compared to the analytical uncertainties associated with isotopic measurements, and no method of calculating the relative pressure corrections for each mineral is available by this method.

A second method for estimating the pressure effects on oxygen isotope fractionation between minerals can be made by comparing the electrostatic site potentials of oxygen in minerals at high pressure. High pressure structures have been determined at room temperature for quartz, coesite, diopside, andalusite and pyrope (references in Table 6). Unfortunately, high pressure structure data were not found for kyanite, albite or sanidine. We used these data to compute electrostatic potentials for the average oxygen sites at the pressures of the structure refinements and interpolated the values to 40 kb. These results are given in Table 6 along with the 1 atm values. The small increase in the average oxygen site potentials with pressure for most of the phases will only result in a relative change of less than 0.1‰ at 40 kb. The effect of pressure is such that at 50 kb, the calculated temperatures with the 1 bar temperature coefficients will be about 40 °C too high.

Table 6. Electrostatic site potentials, (V) for average oxygen sites at 1 atm and 40 kb

Mineral	1 atm	40 kb	Ref[a]
Quartz	30.816	30.710	1
Coesite	30.350	30.408	2
Pyrope	27.070	27.281	3
$Gr_{48}Py_{28}Alm_{23}$	26.852	n.d.	
Diopside	27.328	27.444	4
Andalusite	28.143	28.268	5
Kyanite	27.67	n.d.	
Sanidine	29.550	n.d.	

[a] Ref. (all 1 atm data from Smyth (1989). High pressure data from (1) Levien et al. 1980; (2) Levien and Prewitt 1981a; (3) Hazen and Finger 1978; (4) Levien and Prewitt 1981b; (5) Ralph et al. 1984; n.d. not determined

For quartz, the oxygen site potential *decreases* with increasing pressure. This is consistent with a slight increase in the Si-O distance with pressure resulting from a decrease in the Si-O-Si angle and resulting decrease in the Si-Si next-nearest neighbor distance.

Pressure effects on isotopic substitutions have been considered in more detail by Polyakov and Kharlashina (1989) and Heybey and Wand (1989). A method to calculate the volume change for an isotopic substitution ($\Delta V'$) has been proposed (Heybey and Wand 1989) such that

$$\Delta V' = -R(\Gamma)/T \ (\text{cm}^3/\text{mol}) \quad (12)$$

where

$$\Gamma = 2\gamma Ao/K \quad (K^2/bar) \quad (13).$$

The effect of pressure on the isotopic fractionation between phase i and j can be denoted as

$$d(1000 \ln \alpha_{i-j})/dP = (\Gamma_i - \Gamma_j)(P-1)/T^2 \quad (14)$$

where γ = Grüneisen parameter, κ = bulk modulus (bars), T = temperature (K), R = gas constant (83.143 cm^3·bar/mol·K) and Ao is related to the reduced partition function by the relation

$$1000 \ln Q = Ao/T^2. \quad (15)$$

Table 7. Physical constants of mineral phases required for the calculation of the pressure effect on isotopic fractionation between phases. Data applicable to Eqs. 14 and 18 in text

Phase	k (mbar)	Ref.	γ (calc)	$Ao \times 10^{-6}$ (K^2)	Ref.	Cp^1 (J/mol·K)	V^0 (J/bar)	$\alpha \times 10^6$ (°C)	Ref.	Γ K^2·mol/bar	qz-min (at 1200 °C, 40 kb)	coe-min	py-min
Quartz	0.37	1	0.64	11.7	10	44.59	2.27	34	16	40.5			
Coesite	1.14	2	0.41	11.7	11	45.40	2.06	8	16	8.5	0.59		
Pyrope	1.75	3	1.16	8.9	12	325.50	11.32	19	16	11.8	0.53	−0.06	
Diopside	1.13	4	1.08	9.0	10	166.50	6.62	24	16	17.3	0.43	−0.16	−0.10
Sanidine	0.67	5	0.50	10.8	10	204.50	10.9	14	16	16.1	0.45	−0.14	−0.08
Kyanite	0.43	6	0.17	10.0	13	121.70	4.41	11	16	8.0	0.60	0.01	0.07
Jadeite	1.43	7	1.08	8.0	14	160.00	6.03	20	16	12.1	0.52	−0.06	−0.01
Calcite	0.73	8	0.29	11.4	10	83.47	3.69	9	17	9.1	0.58	−0.01	0.05
Rutile	2.16	9	1.84	6.9	15	55.10	1.88	25	17	11.8	0.53	−0.06	−0.00

Ref. (1) Bass et al. 1981; (2) Weidner and Carleton 1977; (3) Leitner et al. 1980; (4) Levien et al. 1979; (5) Angel et al. 1988; (6) Brace et al. 1969; (7) Kandelin and Weidner 1988; (8) Birch 1966; (9) Hazen and Finger 1981; (10) Clayton and Kieffer 1991; (11) assumed equal to quartz; (12) Lichtenstein and Hoernes 1992; (13) this study; (14) diopside value corrected to jadeite based on relation of Matthews et al. 1983; (15) Agrinier 1991; (16) Skinner 1966; (17) calculated from Berman 1987

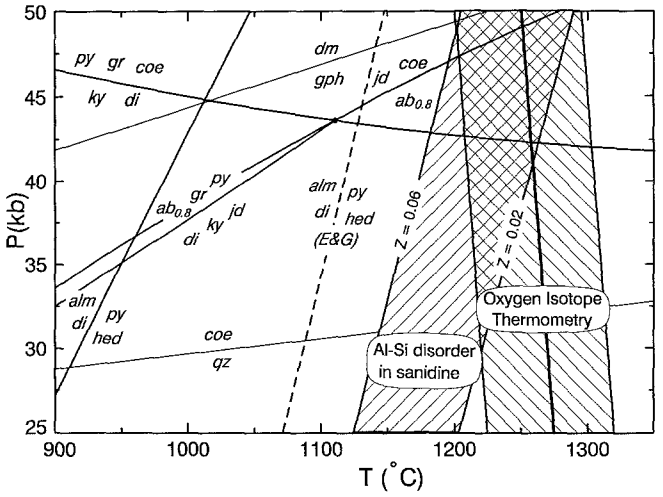

Fig. 8. Combined pressure-temperature estimates from mineral equilibria, Al-Si disorder in sanidine and oxygen isotope thermometry. The errors associated with the oxygen isotope and Al-Si disorder sanidine temperature estimates are shown by the *shaded areas* for each. The pressure-correction for the oxygen isotope data yield a slight negative slope. Abbreviations for mineral equilibria as in Fig. 7, Z = disorder term in sanidine

Equation 14 can be modified using the identity:

$$\gamma = \kappa_s \beta V^0 / Cp \tag{16}$$

to yield

$$\Gamma = 2\beta V^0 Ao / Cp \tag{17}$$

and finally

$$d(1000 \ln \alpha_{i-j})/dP = 2(\beta_i V_i^0 Ao_i / Cp_i - \beta_j V_j^0 Ao_j / Cp_j)(P-1)/T^2. \tag{18}$$

where κ_s is the adiabatic zero pressure bulk modulus, β is the thermal expansivity, V^0 is the molar volume and Cp is the molar heat capacity at constant pressure. A compilation of the necessary constants is given in Table 7. The fractionation between quartz and other minerals due to the pressure increase from 0 to 40 kb at 1200 °C is 0.4–0.7‰. This is a significant effect that would drastically alter the calculated oxygen isotope temperature estimates. The stable polymorph of SiO_2 in sample SRV-1 is not quartz, however, but coesite. The pressure-induced fractionation between coesite and all other phases is less than 0.2‰. Such an effect is small but sufficient to reduce the calculated temperatures by about 50 °C at 50 kb (Fig. 8). This pressure effect is similar to the 40 °C temperature reduction at 50 kb based on the electrostatic site potential data. The pressure effect estimates are certainly not without large errors, but they may offer an explanation in part, for the discrepancy between the cation-based and oxygen isotope thermometers. For high pressure rocks in the quartz stability field, the pressure effect could be significant and should be considered.

Pressure-temperature estimates for the coesite-bearing grospydite

The complete set of pressure-temperature estimates from all methods are presented in Fig. 8. The temperature estimates based on the oxygen isotope fractionations between coesite, sanidine, clinopyroxene and garnet are 1310±80 °C (1 bar). Temperature estimates are 50 °C lower if a pressure correction is applied to the data. These later temperatures are in agreement with those predicted from Al-Si disorder in feldspar. Temperature estimates from Fe-Mg exchange between garnet and clinopyroxene are 1100 °C. The discrepancy between the isotope and cation exchange thermometry requires that either there is an error in one of the estimates or that the different thermometers equilibrated at different temperatures.

The three thermometric calibrations (a, b, c) for oxygen isotope thermometry have been derived by a combination of empirical, theoretical and experimental techniques. All give the same results, and there is no reason to suppose that the calibrations are in error. The temperature estimates based on Eq. 3 have an uncertainty of ±80 to 90 °C. At very high temperatures, total isotopic variations are small, so that the real uncertainty of the isotopic measurements may be close to double this value. It is possible that the isotopic data are, in fact, compatible with the cation exchange thermometry. The coesite data have the largest scatter, and they strongly influence the linear regression used for temperature estimates. If the predicted temperature coefficient of fractionation $a_{qz-coe} = 0.35$ from the data of Smyth (1989) is correct, then the temperature estimates will be 1200 °C instead of 1300 °C. Furthermore, if the highest $\delta^{18}O_{coesite} = 9.05‰$ is actually the correct value, then the linear regression of all data by Eq. 3 will be 1100 °C, in agreement with the cation exchange thermometry.

The cation exchange thermometry estimates also have large uncertainties. The experimental calibration of Ellis and Green (1979) is valid only for Ca-poor garnets. For calcium-rich garnets, the garnet-clinopyroxene exchange thermometer is over extrapolated and may have a large error (Essene 1989). A further possibility for the discrepancy between the garnet-clinopyroxene exchange thermometer and the isotope thermometers is that there has been partial reequilibration of the former during retrogression. In this case, while the calibrations for both the isotope and cation-exchange thermometers may be correct, the garnet-clinopyroxene Fe-Mg exchange thermometer is recording cooling, rather than peak, metamorphic temperatures. A best overall estimate for equilibration temperatures is considered to be 1200±100 °C. This temperature is intermediate to the oxygen isotope estimates and garnet-clinopyroxene estimates, and equal to the estimate based on the Al-Si disorder in sanidine.

Pressure-temperature-time paths

The peak temperatures and pressures of formation for sample SRV-1 are 1200±100 °C and 45±5 kb. The retrograde zoning profile in the sanidine (Fig. 2) indicates formation of a more Na-rich feldspar from jadeite and coesite (or quartz) by reactions 7 and 10 at a pressure of 25–30 kb. The coesite-quartz inversion also occurs in this pressure range. This decompression must have been

close to isothermal. Otherwise, a Fe-Mg zoning profile would have developed between garnet and clinopyroxene and the sanidine would have become more ordered. Experimental determinations of the anhydrous solidus of quartz eclogite (Green and Ringwood 1967; Ito and Kennedy 1971) are well above 1300 °C at 40 kb and about 1250 °C at 25 kb (Fig. 7). Melting experiments of quartz eclogite with excess H_2O place the liquidus at approximately 1100 °C at 40 kb (Lambert and Wyllie 1972; Stern et al. 1975), well below the temperatures recorded by sample SRV-1 (Fig. 7). Rapid decompression of the coesite – sanidine eclogite does not require partial melting as long as the sample was free of H_2O.

The preservation of disordered sanidine in the coesite-sanidine grospydite is difficult to explain unless the xenolith was sampled while at or near equilibrium. A similar conclusion has also been reached for some deep crustal xenoliths (Hayob et al. 1989), although the inference is controversial (Harley 1990; Harte and Barnicoat 1990 vs. Hayob et al. 1990). In the case of the Roberts Victor kimberlites, the inference yields a point on the upper Cretaceous geotherm in Southern Africa. The *P-T* conditions from sample SRV-1 lie on the geotherm of Carswell and Gibb (1987) for Lesotho garnet peridotites, but are at somewhat higher temperatures than that obtained with a typical continental shield geotherm calculated for a 40 mW/m^2 surface heat flow (Pollack and Chapman 1977). It may be dangerous to generally rely on xenoliths transported in kimberlites for average geothermal conditions because the portions of the mantle that produce kimberlites may be anomalously heated by a plume (Irving 1976). Nonetheless, we propose that the 45 ± 5 kb and 1200 ± 100 °C recorded in the xenolith represent conditions extant in the upper mantle shortly before the grospydite became entrained in the kimberlite eruptive.

Source rock and tectonic implications

The process of grospydite and eclogite formation is enigmatic. The unusual chemistry of grospydites, in particular, and eclogites, in general, has been explained in terms of high pressure fractional crystallization from primary mantle melts or melts of subducted material (e.g., Lappin 1978; Smyth et al. 1989) or as prograde metamorphic products of subducted oceanic crust (e.g., Jagoutz et al. 1984; MacGregor and Manton 1986; Shervais et al. 1988).

Oxygen isotope compositions of mantle xenoliths provide some of the most indisputable evidence for subducted material being the ultimate source, but do not shed light on whether the formation process was high pressure accumulation of hyper-aluminous clinopyroxene (Smyth et al. 1989) or low pressure accumulation of plagioclase (MacGregor and Manton 1986; Shervais et al. 1988). The $\delta^{18}O$ value of uncontaminated mantle has a maximum range of 5 to 7‰ (Kyser et al. 1982; Kyser 1986). Samples lying outside this range are best explained by recycling of oceanic crust. Previous measurements of the $\delta^{18}O$ values of grospydites are in the range of pristine mantle (Garlick et al. 1971; MacGregor and Manton 1986 – sample no. 53). The calculated whole rock $\delta^{18}O$ value of 7.7‰ for this coesite-bearing grospydite is outside the primary mantle range and is consistent with its derivation from subducted altered oceanic basalt. Pressure estimates for the grospydite SRV-1 correspond to equilibration depth of 150–160 km; subduction of oceanic crust has therefore occurred into the asthenosphere.

The oxygen isotope thermometric estimates in this study are the highest measured to date. The preservation of such high temperatures is due to the extremely refractory behavior of the grospydite mineral assemblage combined with a rapid quenching from peak temperatures. Oxygen isotope thermometry of refractory phases has previously been limited by the difficulty in fluorination of such materials (e.g., Kyser 1986). The limited and scattered data on kyanite confirm this problem. Recent advances in laser-based analytical techniques allow for the analysis of extremely refractory phases. Further oxygen isotope geochemical studies of ultra-refractory phases, such as garnet, olivine, coesite, kyanite, corundum and staurolite are expected to preserve peak temperature chemistries even when other phases have partially reset. Stable isotope thermometry may prove, in fact, to be one of the most robust thermometers in high temperature systems, as long as the appropriate mineralogy and mineral phases are chosen for analysis.

Acknowledgements. The operating costs for the Stable Isotope Laboratory were provided for by a Swiss National Science Foundation Grant to JC Hunziker and ZD Sharp. EJ Essene was supported by US NSF Grant EAR 91-17772, and JR Smyth by US NSF Grant EAR 91-05391. JC Hunziker has provided assistance and ideas throughout. F Bussy is thanked for instruction on the electron microprobe. The reviews of T Chacko, MA Cosca, S Hoernes and SW Sharp were very much appreciated and improved the manuscript.

References

Afifi A, Essene EJ (1988) MINFILE: a microcomputer program for storage and manipulation of chemical data on minerals. Am Mineral 73:446–448

Agrinier P (1991) The natural calibration of $^{18}O/^{16}O$ geothermometers: application to the quartz-rutile mineral pair. Chem Geol 91:49–64

Anderson AT Jr, Clayton RN, Mayeda TK (1971) Oxygen isotope thermometry of mafic igneous rocks. J Geol 79:715–729

Angel RJ, Hazen RM, McCormick TC, Prewitt CT, Smyth JR (1988) Comparative compressibility of end-member feldspars. Phys Chem Mineral 15:313–318

Anovitz LM (1991) Al zoning in pyroxene and plagioclase: window on late prograde to early retrograde P – T paths in granulite terranes. Am Mineral 76:1328–1343

Anovitz LM, Essene EJ (1987) Compatibility of geobarometers in the system $CaO\text{-}FeO\text{-}Al_2O_3\text{-}SiO_2\text{-}TiO_2$ (CFAST): implications for garnet mixing models. J Geol 95:633–645

Bass JD, Liebermann RC, Weidner DJ, Finch SJ (1981) Elastic properties from acoustic and volume compression experiments. Phys Chem Planet Inter 25:140–158

Berman RG (1987) Internally-consistent thermodynamic data for minerals in the system $Na_2O\text{-}K_2O\text{-}CaO\text{-}MgO\text{-}FeO\text{-}Fe_2O_3\text{-}Al_2O_3\text{-}SiO_2\text{-}TiO_2\text{-}H_2O\text{-}CO_2$. J Petrol 29:445–522

Berman RG (1990) Mixing properties of Ca-Mg-Fe-Mn garnets. Am Mineral 75:328–344

Birch F (1966) Compressibility: elastic constants. In: Clark SP Jr (ed) Handbook of physical constants. Geol Soc Amer Mem 97:97–174

Bohlen SR, Boettcher AL (1982) The quartz=coesite transformation: a precise determination and the effects of other components. J Geophys Res 87:7073–7078

Bottinga Y, Javoy M (1973) Comments on oxygen isotope geothermometry. Earth Planet Sci Lett 20:250–265

Bottinga Y, Javoy M (1975) Oxygen isotope partitioning among the minerals in igneous and metamorphic rocks. Rev Geophys Space Phys 13:401–418

Boyd FR (1973) A pyroxene geotherm. Geochim Cosmochim Acta 37:2533–2546

Boyd FR, Nixon PH (1973) Structure of the upper mantle beneath Lesotho, Carnegie Inst Washington Yearb 74:519–525

Brace WF, Scholz CH, LaMori PN (1969) Isothermal compressibility of kyanite, andalusite and sillimanite from synthetic aggregates. J Geophys Res 74:2089–2098

Caporuscio FA (1990) Oxygen isotope systematics of eclogite mineral phases from South Africa. Lithos 25:203–210

Carswell DA, Gibb FGF (1987) Garnet lherzolite xenoliths in the kimberlites of northern Lesotho: revised P–T equilibration conditions and upper mantle Palaeogeotherm. Contrib Mineral Petrol 97:473–487

Chiba H, Chacko T, Clayton RN, Goldsmith JR (1989) Oxygen isotope fractionations involving diopside, forsterite, magnetite, and calcite: application to geothermometry. Geochim Cosmochin Acta 53:2985–2995

Clayton RN (1981) Isotopic thermometry. In: Newton RC, Navrotsky A, Wood BJ (eds) Thermodynamics of minerals and melts. Springer, Berlin Heidelberg New York, pp 85–109

Clayton RN, Epstein S (1961) The use of oxygen isotopes in high temperature geological thermometry. J Geol 69:447–452

Clayton RN, Kieffer SW (1991) Oxygen isotope thermometer calibrations. In: Taylor HP Jr, O'Neil JR, Kaplan IR (eds) Stable isotope geochemistry: a tribute to Samuel Epstein. Geochem Soc Spec Pub 3:3–10

Clayton RN, Mayeda TK (1963) The use of bromine pentafluoride in the extraction of oxygen from oxides and silicates for isotopic analysis. Geochim Cosmochim Acta 27:43–52

Clayton RN, Goldsmith JR, Karels KJ, Mayeda TK, Newton RC (1974) Limits on the effect of pressure on isotopic fractionation. Geochim Cosmochim Acta 39:1197–1201

Clayton RN, Goldsmith JR, Mayeda TK (1989) Oxygen isotope fractionation in quartz, albite, anorthite, and calcite. Geochim Cosmochim Acta 53:725–733

Cohen RE (1986) Thermodynamic solution properties of aluminous clinopyroxenes: nonlinear least squares refinements. Geochim Cosmochim Acta 50:563–576

Ellis DJ, Green DH (1979) An experimental study of the effect of Ca upon garnet-clinopyroxene Fe-Mg exchange equilibria. Contrib Mineral Petrol 71:13–22

Essene EJ (1989) The current status of thermobarometry in metamorphic rocks. In: Daly JS, Cliff RA, Yardley BWD (eds) Evolution of metamorphic belts. Geol Soc Special Publ 43:1–44

Finnerty AA, Boyd FR (1984) Evaluation of thermobarometers for garnet peridotites. Geochim Cosmochim Acta 48:15–27

Finnerty AA, Boyd FR (1987) Thermobarometry for garnet peridotite xenoliths: a basis for upper mantle stratigraphy. In: Nixon PH (ed) Mantle xenoliths. Wiley, Chichester, pp 381–402

Fonarev VI, Graphchikov AA, Konilov AN (1991) A consistent system of geothermometers for metamorphic complexes. Intl Geol Rev 33:743–783

Fuhrman ML, Lindsley DH (1988) Ternary-feldspar modeling and thermometry. Am Mineral 73:201–215

Ganguly J, Saxena SK (1984) Mixing properties of aluminosilicate garnets: constraints from natural and experimental data, and applications to geothermo-barometry. Am Mineral 69:88–97

Garlick GD, Epstein S (1965) Oxygen isotope ratios in coexisting minerals of regionally metamorphosed rocks. Geochim Cosmochim Acta 31:181–214

Garlick GD, MacGregor ID, Vogel DE (1971) Oxygen isotope ratios in eclogites from kimberlites. Science 172:1025–1027

Gasparik T (1984) Experimental study of subsolidus phase relations and mixing properties of pyroxene in the system CaO-Al_2O_3-SiO_2. Geochim Cosmochim Acta 48:2537–2546

Giletti GJ (1986) Diffusion effects on oxygen isotope temperatures of slowly cooled igneous and metamorphic rocks. Earth Planet Sci Lett 77:218–228

Green DH, Ringwood AE (1967) An experimental investigation of the gabbro to eclogite transformation and its petrological applications. Geochim Cosmochim Acta 31:767–833

Harley SL (1990) High-temperature granulites – comment. Nature 347:132–133

Harte B, Barnicoat A (1990) High-temperature granulites – comment. Nature 347:133

Hayob JL, Essene EJ, Ruiz J, Ortega-Gutierrez F, Aranda-Gomez JJ (1989) Young high-temperature granulites from the base of the crust in central Mexico. Nature 342:265–268

Hayob JL, Essene EJ, Ruiz J (1990) High-temperature granulites – reply. Nature 347:133–134

Hazen RM, Finger LW (1978) Crystal structures and compressibilities of pyrope and grossular to 60 kbar. Am Mineral 63:297–303

Hazen RM, Finger LW (1981) Bulk moduli and high-pressure crystal structures of rutile-type compounds. J Phys Chem Solids 42:143–151

Heybey J, Wand U (1989) Effect of pressure on isotope fractionation in the system CaO-MgO-SiO_2-C-H-O. In: Wand U, Strauch G (eds) Isotopes in nature. Fifth Workshop Meeting, Central Institute of Isotope and Radiation Research, Leipzig, pp 723–734

Hoering TC (1961) The effect of physical changes on isotopic fractionation. Carnegie Inst Washington Yearb 61:201–204

Hoernes S, Friedrichsen H (1980) Oxygen and hydrogen isotopic composition of Alpine and Pre-Alpine minerals of the Swiss Central Alps. Contrib Mineral Petrol 72:19–32

Hoernes S, Hoffer E (1979) Equilibrium relations of prograde metamorphic mineral assemblages. Contrib Mineral Petrol 68:377–389

Hoffbauer R, Hoernes S, Fiorentini E (1992) Oxygen isotope thermometry of granulite-grade rocks from Sri Lanka. Precambrian Res (in press)

Holland TJB, Powell R (1990) An enlarged and updated internally consistent thermodynamic dataset with uncertainties and correlations: The system K_2O-Na_2O-CaO-MgO-MnO-FeO-Fe_2O_3-Al_2O_3-TiO_2-SiO_2-C-H_2-O_2. J Metam Geol 8:89–124

Hovis GL (1974) A solution calorimetric and X-ray investigation of Al-Si distribution in monoclinic potassium feldspars. In: MacKenzie WS, Zussman J (eds) The feldspars. Manchester University Press, Manchester, UK, pp 114–144

Hovis GL (1986) Behavior of alkali feldspars: crystallographic properties and characterization of composition and Al-Si disorder. Am Mineral 71:869–890

Irving AJ (1976) On the validity of paleogeotherms determined from xenolith suites in basalts and kimberlites. Am Mineral 61:638–642

Ito K, Kennedy GC (1971) An experimental study of the basalt-garnet granulite-eclogite transitions. In: Heacock JG (ed) The structure and physical properties of the Earth's crust. Am Geophys Union Geophys Mon 14:303–314

Jagoutz E, Dawson JB, Hoernes S, Spettel B, Wanke H (1984) Anorthositic oceanic crust in the Archean. In: The early Earth. Lunar Planet Sci Tech Rep 15:395–396

Javoy M, Fourcade S, Allegre CJ (1970) Graphical method for examination of $^{18}O/^{16}O$ fractionations in silicate rocks. Earth Planet Sci Lett 10:12–16

Kandelin J, Weidner DJ (1988) The single-crystal elastic properties of jadeite. Phys Earth Planet Inter 50:251–260

Kennedy CS, Kennedy GC (1976) The equilibrium boundary between graphite and diamond. J Geophys. Res 81:2467–2470

Kirschner D, Sharp ZD, Tessyier C (1992) In situ oxygen isotope study of en-èchelon quartz veins. Geol (in press)
Krogh EJ (1988) The garnet-clinopyroxene Fe-Mg geothermometer – a reinterpretation of existing experimental data. Contrib Mineral Petrol 99:44–48
Kroll H, Ribbe PH (1983) Lattice parameters, composition, and Al, Si order in alkali feldspars. In: Ribbe PH (ed) Feldspar mineralogy. Mineral Soc Am Rev Mineral 2:57–99
Kyser TK (1986) Stable isotope variations in the mantle. In: Valley JW, Taylor HP Jr, O'Neil JR (eds) Stable isotope in high temperature geological processes. Rev Mineral 16:141–164
Kyser TK, O'Neil JR, Carmichael ISE (1981) Oxygen isotope thermometry of basic lavas and mantle nodules. Contrib Mineral Petrol 77:11–23
Kyser TK, O'Neil JR, Carmichael ISE (1982) Genetic relations among basic lavas and ultramafic nodules.: evidence from oxygen isotope compositions. Contrib Mineral Petrol 81:88–102
Lambert IB, Wyllie PJ (1972) Melting of gabbro (quartz eclogite) with excess water to 35 kilobars, with geological applications. J Geol 80:693–708
Lappin MA (1978) The evolution of a grospydite from the Roberts Victor Mine, South Africa. Contrib Mineral Petrol 66:229–241
Leitner BJ, Weidner DJ, Liebermann RC (1980) Elasticity of single crystal pyrope and implications for garnet solid solution series. Phys Earth Plan Inter 22:111–121
Levien L, Prewitt CT (1981a) High pressure crystal structure and compressibility of coesite. Am Mineral 65:920–930
Levien L, Prewitt CT (1981b) High pressure structural study of diopside. Am Mineral 66:315–323
Levien L, Prewitt CT, Weidner DJ (1980) Structure and elastic properties of quartz at pressure. Am Mineral 65:920–930
Levien L, Weidner DJ, Prewitt CT (1979) Elasticity of diopside. Phys Chem Min 4:105–113
Lichtenstein U, Hoernes S (1992) Oxygen isotope fractionations between grossular-spessartine garnet and water: an experimental investigation. Eur J Mineral 4:239–249
Lindsley DH, Nekvasil H (1989) A ternary feldspar model for all reasons. Eos 70:506
MacGregor ID, Manton WI (1986) Roberts Victor eclogites: ancient oceanic crust. J Geophys Res 91:14063–14079
Matthews A, Goldsmith JR, Clayton RN (1983) Oxygen isotope fractionations involving pyroxenes: the calibration of mineral-pair geothermometers. Geochim Cosmochim Acta 47:631–644
McCormick TC, Smyth JR (1986) Geothermometry and geobarometry for kyanite eclogites from Bellsbank and Roberts Victor kimberlites. Int Mineral Assoc Abstr. Prog 14:169
O'Neil JR (1986) Theoretical and experimental aspects of isotopic fractionation. In: Valley JW, Taylor HP Jr, O'Neil JR (eds) Stable isotopes in high temperature geological processes. Rev Mineral 16:1–40
O'Neil JR, Taylor HP Jr (1967) The oxygen isotope and cation exchange chemistry of feldspar. Am Mineral 52:1414
Ongley JS, Basu AR, Kyser TK (1987) Oxygen isotopes in coexisting garnets, clinopyroxenes and phlogopites from Robert Victor eclogites: implications for petrogenesis and mantle metasomatism. Earth Planet Sci Lett 83:80–84
Onuma N, Clayton RN, Mayeda TK (1970) Apollo 11 rocks: oxygen isotope fractionation between minerals, and an estimate of the temperature of formation. Proc Apollo 11 Lunar Sci Conf 2:1429–1434
Pattison DRM, Newton RC (1989) Reversed experimental calibration of the garnet-clinopyroxene Fe-Mg exchange thermometer. Contrib Mineral Petrol 101:87–103
Pollack HN, Chapman DS (1977) On the regional variation of heat flow, geotherms and lithospheric thickness. Tectonophysics 38:279–296
Polyakov VB, Kharlashina NN (1989) The effect of pressure on the equilibrium isotopic fractionation in solids. In: Wand U, Strauch G (eds) Isotopes in nature. Fifth Workshop Meeting, Central Institute of Isotope and Radiation Research, Leipzig, pp 735–745
Powell R (1985) Regression diagnostics and a robust regression in geothermometer/geobarometer calibration: the garnet-clinopyroxene geothermometer. J Metam Geol 3:231–243
Powell R, Holland TJB (1988) An internally consistent dataset with uncertainties and correlations: 3. Applications to geobarometry, worked examples and a computer program. J Metam Geol 6:173–204
Råheim A, Green DH (1974) Experimental determination of the temperature and pressure dependence of the Fe-Mg partition coefficient for coexisting garnet and clinopyroxene. Contrib Mineral Petrol 48:179–203
Ralph RL, Finger LW, Hazen RM, Ghose S (1984) Compressibility and crystal structure of andalusite at high pressure. Am Mineral 69:513–519
Richter R, Hoernes S (1988) The application of the increment method in comparison with experimentally derived and calculated O-isotope fractionations. Chem Erde 48:1–18
Scambos TA, Smyth JR, McCormick TC (1987) Crystal-structure refinement of high sanidine from the upper mantle. Am Mineral 72:973–978
Sharp ZD (1990) A laser-based microanalytical method for the in situ determination of oxygen isotope ratios in silicates and oxides. Geochim Cosmochim Acta 54:1353–1357
Sharp ZD (1992) In situ laser microprobe techniques for stable isotope analyses. Isotope Geosci 101:3–19
Sharp ZD, O'Neil JR, Essene EJ (1988) Oxygen isotope variations in granulite-grade iron formations: constraints on oxygen diffusion and retrograde isotopic exchange. Contrib Mineral Petrol 98:490–501
Shervais JW, Taylor LA, Lugmair GW, Clayton RN, Mayeda TK, Korotev RL (1988) Early Proterozoic oceanic crust and the evolution of subcontinental mantle: eclogites and related rocks from southern Africa. Geol Soc Am Bull 100:411–423
Skinner BJ (1966) Thermal expansion. In: Clark SP Jr (ed) Handbook of physical constants. Geol Soc Am Mem 97:75–96
Smyth JR (1989) Electrostatic characterization of oxygen sites in minerals. Geochim Cosmochim Acta 53:1101–1110
Smyth JR, Clayton RN (1988) Correlation of oxygen isotope fractionation and electrostatic site potentials in silicates. Eos 69:1514
Smyth JR, Hatton CJ (1977) A coesite – sanidine grospydite from the Robert Victor kimberlite. Earth Planet Sci Lett 77:284–290
Smyth JR, Caporuscio FA, McCormick TC (1989) Mantle eclogites: evidence of igneous fractionation in the mantle. Earth Planet Sci Lett 93:133–141
Stern CR, Huang W-L, Wyllie PJ (1975) Basalt-andesite-rhyolite-H_2O: crystallization intervals with excess H_2O and H_2O-undersaturated liquidus surfaces to 35 kilobars, with implications for magma genesis. Earth Planet Sci Lett 28:189–196
Taylor HP Jr, Epstein S (1970) O^{18}/O^{16} ratios of Apollo 11 lunar rocks and minerals. Proc Apollo 11 Lunar Sci Conf 2:1613–1626
Taylor HP Jr, Albee AL, Epstein S (1963) O^{18}/O^{16} ratios of coexisting minerals in three assemblages of kyanite-zone pelitic schist. J Geol 71:513–522
Thompson JB Jr, Waldbaum DR (1969) Mixing properties of sanidine and crystalline solutions II. Calculations based on two-phase data. Am Mineral 54:811–838
Weidner DJ, Carleton HR (1977) Elasticity of coesite. J Geophys Res 82:1334–1346
Wohletz KH, Smyth JR (1984) Origin of a Roberts Victor sanidine-coesite-grospydite: thermodynamic considerations. In: Kornprobst J (ed) Kimberlites II: the mantle and crust-mantle relationships. Elsevier, Amsterdam, pp 33–42

Editorial responsibility: J. Hoefs